

1 **A new model of decision processing in instrumental learning tasks**

2

3 Steven Miletić<sup>a\*</sup>, Russell J. Boag<sup>a</sup>, Anne C. Trutti<sup>a,b</sup>, Birte U. Forstmann<sup>a</sup>, Andrew Heathcote<sup>a,c</sup>

4

5

6 <sup>a</sup> University of Amsterdam, Department of Psychology, Nieuwe Achtergracht 129B, Amsterdam, The

7 Netherlands

8 <sup>b</sup> Leiden University, Department of Psychology, Wassenaarseweg 52, Leiden, The Netherlands

9 <sup>c</sup> University of Newcastle, School of Psychology, Newcastle, Australia

10

11 \*Correspondence concerning this article should be addressed to Steven Miletić, Nieuwe Achtergracht 129B,

12 1001NK Amsterdam, The Netherlands. E: [s.miletic@uva.nl](mailto:s.miletic@uva.nl)

13

14 **Abstract**

15 Learning and decision making are interactive processes, yet cognitive modelling of error-  
16 driven learning and decision making have largely evolved separately. Recently, evidence  
17 accumulation models (EAMs) of decision making and reinforcement learning (RL) models of  
18 error-driven learning have been combined into joint RL-EAMs that can in principle address  
19 these interactions. However, we show that the most commonly used combination, based on the  
20 diffusion decision model (DDM) for binary choice, consistently fails to capture crucial aspects  
21 of response times observed during reinforcement learning. We propose a new RL-EAM based  
22 on an advantage racing diffusion (ARD) framework for choices among two or more options  
23 that not only addresses this problem but captures stimulus difficulty, speed-accuracy trade-off,  
24 and stimulus-response-mapping reversal effects. The RL-ARD avoids fundamental limitations  
25 imposed by the DDM on addressing effects of absolute values of choices, as well as extensions  
26 beyond binary choice, and provides a computationally tractable basis for wider applications.

27

28 *Keywords:* Decision making, reinforcement learning, evidence-accumulation models, speed-  
29 accuracy trade-off, reversal learning.

30

31

32

33

34 Learning and decision-making are mutually influential cognitive processes. Learning processes  
35 refine the internal preferences and representations that inform decisions, and the outcomes of  
36 decisions underpin feedback-driven learning (Bogacz and Larsen, 2011). Although this relation  
37 between learning and decision-making has been acknowledged (Bogacz and Larsen, 2011;  
38 Dayan and Daw, 2008), the study of cognitive processes underlying feedback-driven learning  
39 on the one hand, and of perceptual and value-based decision-making on the other, have  
40 progressed as largely separate scientific fields. In the study of error-driven learning (O’Doherty  
41 et al., 2017; Sutton and Barto, 2018), the decision process is typically simplified to soft-max,  
42 a descriptive model that offers no process-level understanding of how decisions arise from  
43 representations, and ignores choice response times (RTs). In the study of decision-making  
44 using evidence-accumulation models (EAMs; Donkin and Brown, 2018; Forstmann et al.,  
45 2016; Ratcliff et al., 2016), tasks are typically designed to minimize the influence of learning,  
46 and residual variability caused by learning is treated as noise.

47 Recent advances (Fontanesi et al., 2019a, 2019b; Luzardo et al., 2017; McDougle and  
48 Collins, 2020; Miletic et al., 2020; Millner et al., 2018; Pedersen et al., 2017; Pedersen and  
49 Frank, 2020; Sewell et al., 2019; Sewell and Stallman, 2020; Shahar et al., 2019; Turner, 2019)  
50 have emphasized how both modelling traditions can be combined in joint models of  
51 reinforcement learning (RL) and evidence-accumulation decision-making processes, providing  
52 mutual benefits for both fields. Combined models generally propose that value-based decision-  
53 making and learning interact as follows: For each decision a subject gradually accumulates  
54 evidence for each choice option by sampling from a distribution of memory representations of  
55 the subjective value (or *expected reward*) associated with each choice option (known as *Q-*  
56 *values*). Once a threshold level of evidence is reached, they commit to the decision and initiate  
57 a corresponding motor process. The response triggers feedback, which is used to update the  
58 internal representation of subjective values. The next time the subject encounters the same  
59 choice options, this updated internal representation changes evidence accumulation.

60 The RL-EAM framework has many benefits (Miletic et al., 2020). It allows for studying a  
61 rich set of behavioral data simultaneously, including entire RT distributions and trial-by-trial  
62 dependencies in choices and RTs. It posits a theory of evidence accumulation that assumes a  
63 memory representation of rewards is the source of evidence, and it formalizes how these  
64 memory representations change due to learning. It complements earlier work connecting  
65 theories of reinforcement learning and decision-making (Bogacz and Larsen, 2011; Dayan and  
66 Daw, 2008) and their potential neural implementation in basal ganglia circuits (Bogacz and  
67 Larsen, 2011), by presenting a measurement model that can be fit to, and makes predictions  
68 about, behavioral data. Adding to benefits in terms of theory building, the RL-EAM framework  
69 also has potential to improve parameter recovery properties compared to standard RL models  
70 (Shahar et al., 2019), and allows for the estimation of single-trial parameters of the decision  
71 model, which can be crucial in the analysis of neuroimaging data.

72 An important challenge of this framework is the number of modeling options in both the  
73 fields of reinforcement learning and decision-making. Even considering only model-free (as  
74 opposed to model-based (Daw and Dayan, 2014)) reinforcement learning, there exists a variety  
75 of learning rules (e.g., Palminteri et al., 2015; Rescorla and Wagner, 1972; Rummery and  
76 Niranjan, 1994; Sutton, Richard, 1988), as well as the possibility of multiple learning rates for  
77 positive and negative prediction errors (Christakou et al., 2013; Daw et al., 2002; Frank et al.,

78 2009; Gershman, 2015; Haughey et al., 2007; Niv et al., 2012), and many additional concepts,  
79 such as eligibility traces to allow for updating of previously visited states (Barto et al., 1981;  
80 Bogacz et al., 2007). Similarly, in the decision-making literature, there exists a wide range of  
81 evidence-accumulation models, including most prominently the diffusion decision model  
82 (DDM; Ratcliff, 1978; Ratcliff et al., 2016) and race models such as the linear ballistic  
83 accumulator model (LBA; Brown and Heathcote, 2008) and racing diffusion (RD) models  
84 (Boucher et al., 2007; Hawkins and Heathcote, 2020; Leite and Ratcliff, 2010; Logan et al.,  
85 2014; Purcell et al., 2010; Ratcliff et al., 2011; Tillman et al., 2020).

86 The existence of this wide variety of modelling options is a double-edged sword. On the one  
87 hand, it highlights the success of the general principles underlying both modelling traditions  
88 (i.e., learning from prediction errors and accumulate-to-threshold decisions) in explaining  
89 behavior, and it allows for studying specific learning/decision-making phenomena. On the  
90 other hand, it constitutes a bewildering combinatorial explosion of potential RL-EAMs; here  
91 we provide empirical grounds to navigate this problem with respect to EAMs.

92 The DDM is the dominant EAM as currently used in reinforcement learning (Fontanesi et  
93 al., 2019a, 2019b; Millner et al., 2018; Pedersen et al., 2017; Pedersen and Frank, 2020; Sewell  
94 et al., 2019; Sewell and Stallman, 2020; Shahar et al., 2019), but this choice is without  
95 experimental justification. Furthermore, the DDM has several theoretical drawbacks, such as  
96 its inability to explain multi-alternative decision-making and its strong commitment to the  
97 accumulation of the evidence *difference*, which leads to difficulties in explaining behavioral  
98 effects of absolute stimulus and reward magnitudes without additional mechanisms (Fontanesi  
99 et al., 2019a; Ratcliff et al., 2018; Teodorescu et al., 2016). Here, we compare the performance  
100 of different decision-making models in explaining choice behavior in a variety of instrumental  
101 learning tasks. Models that fail to capture crucial aspects of performance run the risk of  
102 producing misleading psychological inferences. For EAMs, the full RT distribution (i.e., its  
103 level of variability and skew) have proven to be crucial. Hence, it is important to assess which  
104 RL-EAMs are able to capture not only learning-related changes in choice probabilities and  
105 mean RT, but also the general shape of the entire RT distribution and how it changes with  
106 learning. Further, in order to be held forth as a general modeling framework, it is important to  
107 capture how all of these measures interact with key phenomena in the decision-making and  
108 learning literature.

109 We compare the RL-DDM with two RL-EAMs based on a racing accumulator architecture  
110 (Figure 1). All RL-EAMs assume evidence accumulation is driven by Q-values, which change  
111 based on error-driven learning as governed by the classical State-Action-Reward-State-Action  
112 (SARSA; Rummery and Niranjana, 1994) update rule. Rather than a two-sided DDM process  
113 (Figure 1A), the alternative models adopt a neurally plausible RD architecture (Ratcliff et al.,  
114 2007), which conceptualize decision making as a statistically independent race between single-  
115 sided diffusive accumulators, each collecting evidence for a different choice option. The first  
116 accumulator to reach its threshold triggers motor processes that execute the corresponding  
117 decision. The alternative models differ in how the mean values of evidence are constituted. The  
118 first model, the RL-RD (Figure 1B), postulates accumulators are driven by the expected reward  
119 for their choice, plus a stimulus-independent baseline (c.f. an *urgency* signal; Miletic and Van  
120 Maanen, 2019). The second model, the RL-ARD (advantage racing diffusion), uses the recently  
121 proposed *advantage* framework (Van Ravenzwaaij et al., 2020), assuming that each

122 accumulator is driven by weighted combination of three terms: the *difference* (“advantage”) in  
 123 mean reward expectancy of one choice option over the other, the *sum* of the mean reward  
 124 expectancies, and the urgency signal. In perceptual choice the advantage term consistently  
 125 dominates the sum term by an order of magnitude (Van Ravenzwaaij et al., 2020), but the sum  
 126 term is necessary to explain the effects of absolute stimulus magnitude. We also fit a limited  
 127 version of this model, RL-IARD, with the weight of the sum term set to zero to test whether  
 128 accounting for the influence of the sum is necessary even when reward magnitude is not  
 129 manipulated, as was the case in our experiments. The importance of sum and advantage terms  
 130 is also quantified by their weights as estimated in full RL-ARD model fits.

131 For all models, we first test how well they account for RT distributions (central tendency,  
 132 variability, and skewness of RTs), accuracies, and learning-related changes in RT distributions  
 133 and accuracies in a typical instrumental learning task (Frank, 2004). In this experiment we also  
 134 manipulated difficulty, that is, the magnitude of the difference in average reward between pairs  
 135 of options. In two further experiments we test the ability of the RL-EAMs to capture key  
 136 behavioral phenomena in the decision-making and reinforcement-learning literatures,  
 137 respectively, speed-accuracy trade-off (SAT), and reversals in reward contingencies. Again,  
 138 these tests required a comprehensive account of not only choice probabilities but also the full  
 139 distribution of RT, and learning-related changes thereof.

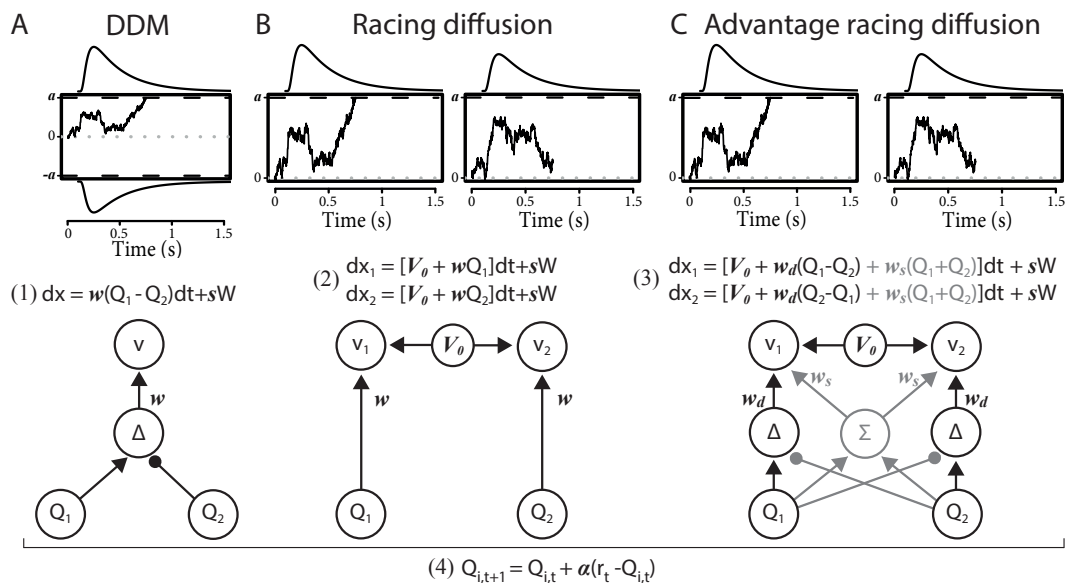


Figure 1. Comparison of the decision-making models. Bottom graphs visualize how Q-values are linked to accumulation rates. Top panel illustrates the evidence-accumulation process of the DDM (panel A) and racing diffusion (RD) models (panels B and C). Note that in the race models there is no lower bound. Equations 1-3 formally link Q-values to evidence-accumulation rates. In the RL-DDM, the difference ( $\Delta$ ) in Q-values is accumulated, weighted by free parameter  $w$ , plus additive within-trial white noise  $W$  with standard deviation  $s$ . In the RL-RD, the (weighted) Q-values for both choice options are independently accumulated. An evidence-independent baseline urgency term,  $V_0$  (equal for all accumulators), further drives evidence accumulation. In the RL-ARD models, the advantages ( $\Delta$ ) in Q-values are accumulated as well, plus the evidence-independent baseline term  $V_0$ . The grey icons indicate the influence of the Q-value *sum* ( $\Sigma$ ) on evidence accumulation, which is not included in the limited variant of the RL-ARD. In all panels, bold-italic faced characters indicate parameters.  $Q_1$  and  $Q_2$  are Q-values for both choice options, which are updated according to a SARSA learning rule (equation (4) at the bottom of the graph), with learning rate  $\alpha$ .

140

141 **Results**

142 In the first experiment, participants made decisions between four sets of two abstract choice  
143 stimuli, each associated with a fixed reward probability (Figure 2A). On each trial, one choice  
144 option always had a higher expected reward than the other; we refer to this choice as the  
145 ‘correct’ choice. After each choice, participants received feedback in the form of points.  
146 Reward probabilities, and therefore choice difficulty, differed between the four sets (Figure  
147 2B). In total, data from 55 subjects were included in the analysis, each performing 208 trials  
148 (see methods).

149 Throughout, we summarize RT distributions by calculating the 10<sup>th</sup>, 50<sup>th</sup> (median) and 90<sup>th</sup>  
150 percentiles separately for correct and error responses. The median summarizes central  
151 tendency, the difference between 10<sup>th</sup> and 90<sup>th</sup> percentiles summarizes variability and the larger  
152 difference between the 90<sup>th</sup> and 50<sup>th</sup> percentiles than between the 50<sup>th</sup> and 10<sup>th</sup> percentiles  
153 summarizes the positive skew that is always observed in RT distributions. To visualize the  
154 effect of learning, we divided all trials in 10 bins (approximately 20 trials each), and calculated  
155 accuracy and the RT percentiles per bin. Note that model fitting was not based on these data  
156 summaries. Instead, we used hierarchical Bayesian methods to fit models to the data from every  
157 trial and participant simultaneously. We compared model fits informally using posterior  
158 predictive distributions—calculating the same summary statistics on data generated from the  
159 fitted model as we did for the empirical data—and formally using the Bayesian Predictive  
160 Information Criterion (BPIC; Ando, 2007). The former method allows us to assess the absolute  
161 quality of fit (Palminteri et al., 2017) and detect misfits; the latter provides a model-selection  
162 criterion that trades off quality of fit with model complexity (lower BPICs are preferred),  
163 ensuring that a better fit is not only due to greater model flexibility.  
164

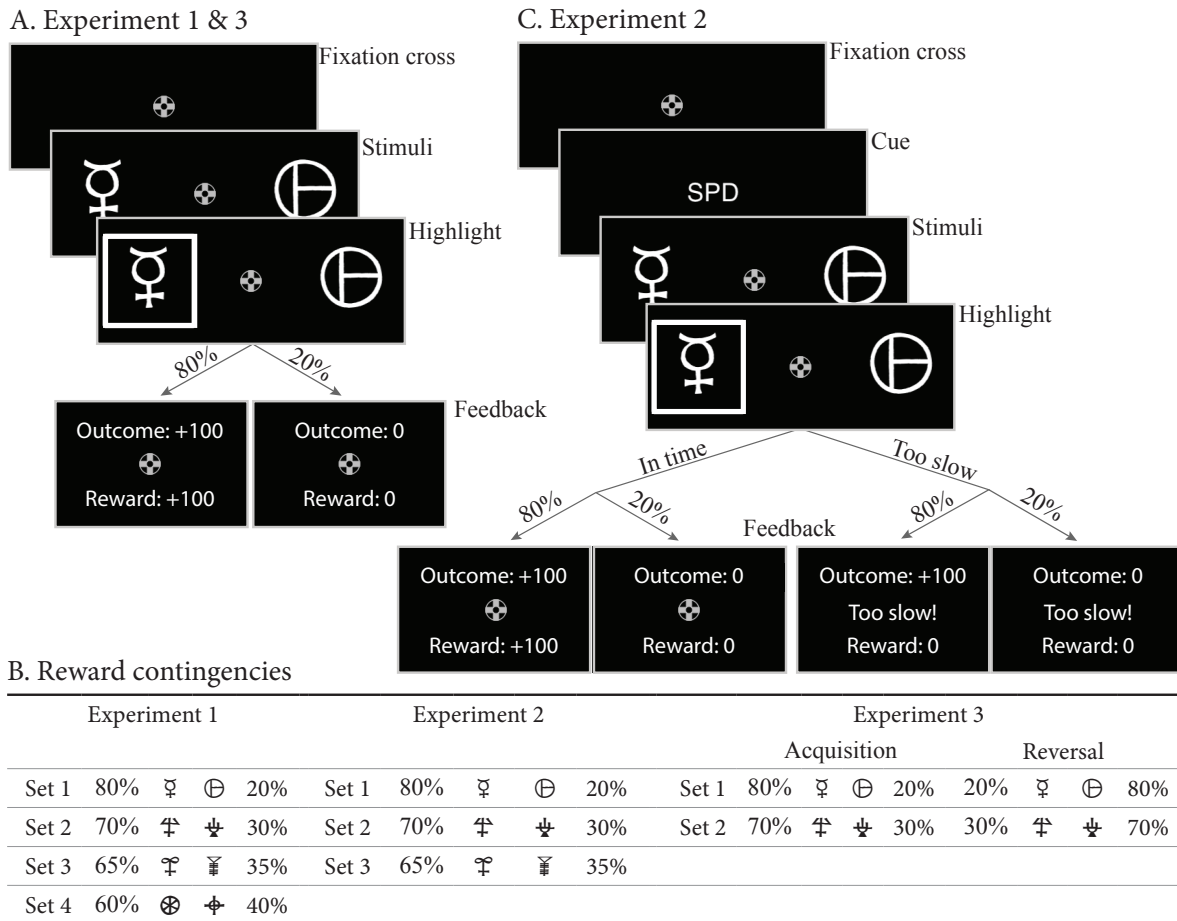


Figure 2. Paradigms for all experiments. A: Example trial for experiment 1 and 3. Each trial starts with a fixation cross, followed by the presentation of the stimulus (until choice is made or 2.5 s elapses), a brief highlight of the chosen option, and probabilistic feedback. Reward probabilities are summarized in B. Percentages indicate the probabilities of receiving +100 points for a choice (with 0 otherwise). The actual symbols used differed between experiments and participants. In experiment 3, the acquisition phase lasted 61-68 trials (uniformly sampled each block), after which the reward contingencies for each stimulus set reversed. C: Example trial for experiment 2, which added a cue prior to each trial ('SPD' or 'ACC'), and had feedback contingent on both the choice and choice timing. In the SPD condition, RTs under 700 ms were considered in time, and too slow otherwise. In the ACC condition, choices were in time as long as they were made in the stimulus window of 1.5 s. Positive feedback "Outcome: +100" and "Reward: +100" were shown in green letters, negative feedback ("Outcome: 0", "Reward: 0", and "Too slow!") were shown in red letters.

165

166 We first examine results aggregated over difficulty conditions. The posterior predictives of all  
 167 four RL-EAMs are shown in Figure 3, with the top row showing accuracies, and the middle  
 168 and bottom rows correct and error RT distributions (parameter estimates for all models can be  
 169 found in the supplementary materials). The RL-DDM generally explains the learning-related  
 170 increase in accuracy well, and if only the central tendency were relevant it might be considered  
 171 to provide an adequate account of RT, although correct median RT is systematically under-  
 172 estimated. However, RT variability and skew are severely over-estimated. The RL-RD largely  
 173 overcomes the RT distribution misfit, but it overestimates RTs in the first trial bins, and while  
 174 capturing an increase in accuracy over trials, it is systematically underestimated. The RL-ARD

175 models provide the best explanation of all key aspects of the data: except for a slight  
176 underestimation of accuracy in early trial bins (largely shared with the RL-DDM), they capture  
177 accuracy well, and like the RL-RD, they capture the RT distributions well, but without  
178 overpredicting the RTs in the early trials. The two RL-ARD models do not differ greatly in fit,  
179 except that the limited version slightly underestimates the decrease in RT with learning.  
180

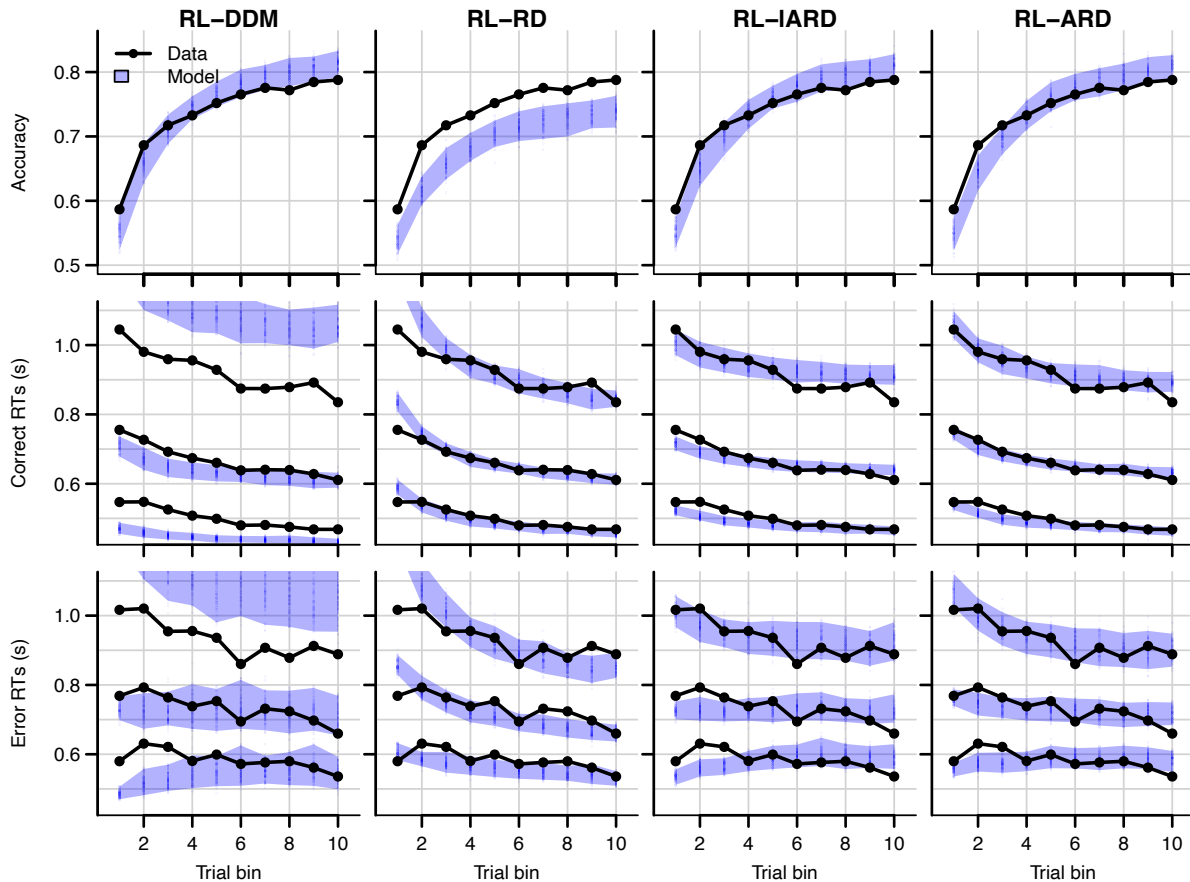


Figure 3. Comparison of posterior predictive distributions of the four RL-EAMs. Data (black) and posterior predictive distribution (blue) of the RL-DDM (left column), RL-RD, RL-IARD, and RL-ARD (right column). Top row depicts accuracy over trial bins. Middle and bottom row show 10<sup>th</sup>, 50<sup>th</sup> and 90<sup>th</sup> RT percentiles for the correct (middle row) and error (bottom row) response over trial bins. Shaded areas correspond to the 95% credible interval of the posterior predictive distributions. All data are collapsed across participants and difficulty conditions.

181

182

183



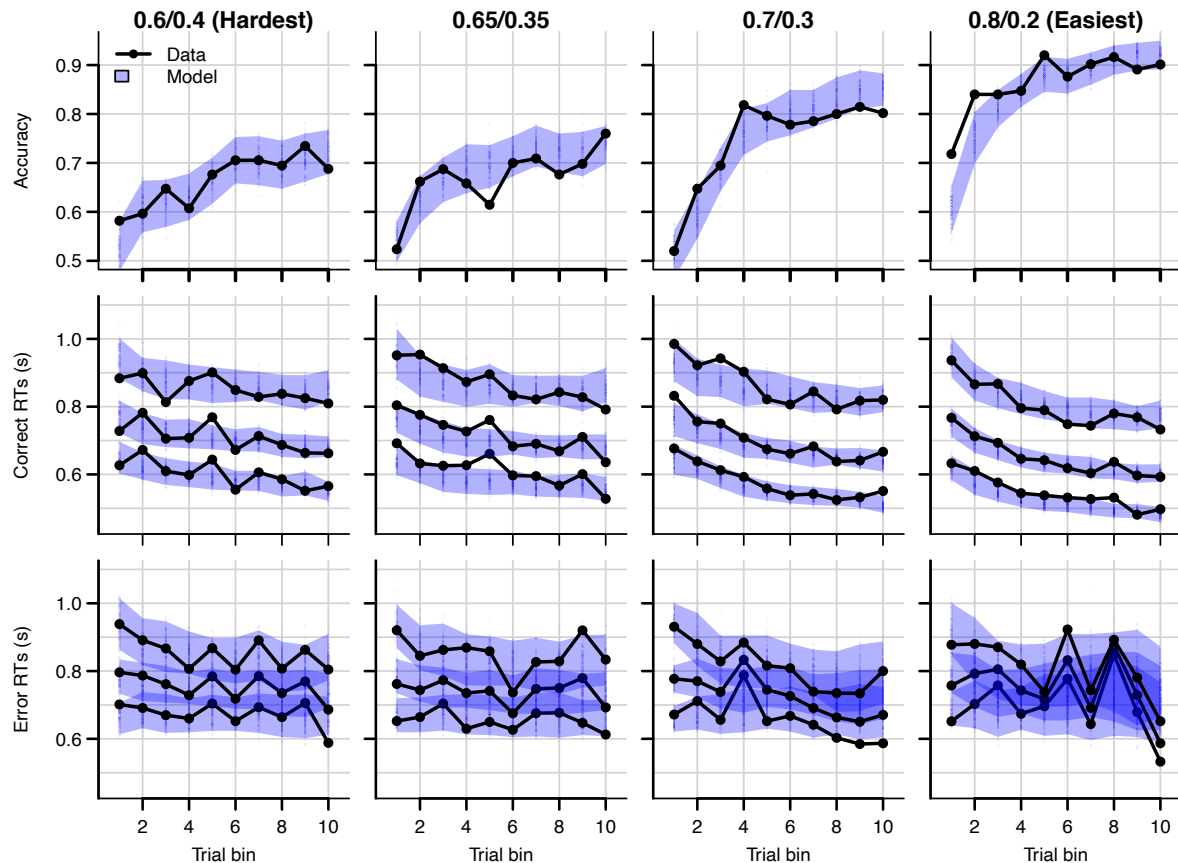


Figure 4. Data (black) and posterior predictive distribution of the RL-ARD (blue), separately for each difficulty condition. Column titles indicate the reward probabilities, with 0.6/0.4 being the most difficult, and 0.8/0.2 the easiest condition. Top row depicts accuracy over trial bins. Middle and bottom rows show 10<sup>th</sup>, 50<sup>th</sup> and 90<sup>th</sup> RT percentiles for the correct (middle row) and error (bottom row) response over trial bins. Shaded areas correspond to the 95% credible interval of the posterior predictive distributions. All data and fits are collapsed across participants.

184

185 Figure 4 shows the data and RL-ARD model fit separated by difficulty (see supplementary  
 186 materials for equivalent RL-DDM fits, which again fail to capture RT distributions). The RL-  
 187 ARD model displays the same excellent fit as to data aggregated over difficulty, except that it  
 188 underestimates accuracy in early trials in the easiest condition (Figure 4, bottom right panel).  
 189 Further inspections of the data revealed that 17 participants (31%) reached perfect accuracy in  
 190 the first bin in this condition. Likely, they guessed correctly on the first occurrence of the  
 191 easiest choice pair, repeated their choice, and received too little negative feedback in the next  
 192 repetitions to change their choice strategy. Supplementary materials show that, with these 17  
 193 participants removed, the overestimation is largely mitigated. SARSA assumes learning from  
 194 feedback, and so cannot explain such high early accuracies. Working memory processes could  
 195 have aided performance in the easiest condition, since the total number of stimuli pairs was  
 196 limited and feedback was quite reliable, making it relatively easy to remember correct-choice  
 197 options (Collins and Frank, 2012a, 2018; McDougle and Collins, 2020).

198

199 **Reward magnitude and Q-value evolution**

200 Q-values represent the participants' internal beliefs about how rewarding each choice option  
201 is. The RL-IARD and RL-DDM assume drift rates are driven only by the difference in Q-values  
202 (Figure 5), and both underestimate the learning-related decrease in RTs. Similar RL-DDM  
203 underestimation has been detected before (Pedersen et al., 2017), with the proposed remedy  
204 being a decrease in the decision bound with time (but with no account of RT distributions).  
205 The RL-ARD explains the additional speed-up through the increasing *sum* of Q-values over  
206 trials (Figure 5C), which in turn increases drift rates (Figure 5D). In line with observations in  
207 perceptual decision-making (Van Ravenzwaaij et al., 2020), the effect of the expected reward  
208 magnitude on drift rate is smaller (on average,  $w_s = 0.36$ ) than that of the Q-value difference  
209 ( $w_D = 2.25$ ) and the urgency signal ( $V_0 = 2.45$ ). Earlier work using an RL-DDM (Fontanesi  
210 et al., 2019a) showed that higher reward magnitudes decrease RTs in reinforcement learning  
211 paradigms. There, the reward magnitude effect on RT was accounted for by allowing the  
212 threshold to change as a function of magnitude. However, this requires participants to rapidly  
213 adjust their threshold based on the identity of the stimuli, something that is usually not  
214 considered possible in EAMs (Donkin et al., 2011; Ratcliff, 1978). The RL-ARD avoids this  
215 problem, with magnitude effects entirely mediated by drift rates, and our result show expected  
216 reward magnitudes influence RTs due to learning even in the absence of a reward magnitude  
217 manipulation. Because the sum affects each accumulator equally, it changes RT with little  
218 effect on accuracy.

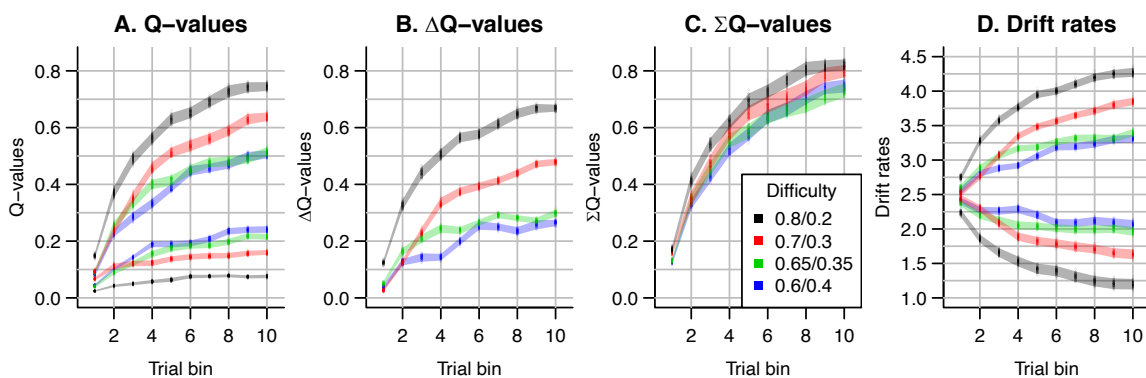


Figure 5. The evolution of Q-values and their effect on drift rates in the RL-ARD. A depicts raw Q-values, separate for each difficulty condition (colors). B and C depict the Q-value differences and the Q-value sums over time. The drift rates (D) are a weighted sum of the Q-value differences and Q-value sums, plus an intercept.

219

## 220 Speed-accuracy trade-off

221 Speed-accuracy trade-off (SAT) refers to the ability to strategically trade-off decision speed  
222 for decision accuracy (Bogacz et al., 2010; Pachella and Pew, 1968; Ratcliff and Rouder,  
223 1998). As participants can voluntarily trade speed for accuracy, RT and accuracy are not  
224 independent variables, so analysis methods considering only one of these variables while  
225 ignoring the other (e.g., soft-max, which only focuses on choice accuracy) can be misleading.  
226 EAMs simultaneously consider RTs and accuracy and allow for estimation of SAT settings.  
227 The classical explanation in the DDM framework (Ratcliff and Rouder, 1998) holds that  
228 participants adjust their SAT by changing the decision threshold: increasing thresholds require  
229 a participant to accumulate more evidence, leading to slower but more accurate responses.

230 Empirical work draws a more complex picture. Several papers suggest that in addition to  
231 thresholds, drift rates (Arnold et al., 2015; Heathcote and Love, 2012; Ho et al., 2012; Rae et  
232 al., 2014; Sewell and Stallman, 2020) and sometimes even non-decision times (Arnold et al.,  
233 2015; Voss et al., 2004) can be affected. Increases in drift rates in a race model could indicate  
234 an urgency signal, implemented by drift gain modulation, with qualitatively similar effects to  
235 collapsing thresholds over the course of a decision (Cisek et al., 2009; Hawkins et al., 2015;  
236 Miletic, 2016; Miletic and Van Maanen, 2019; Murphy et al., 2016; Thura and Cisek, 2016;  
237 Trueblood et al., 2020; van Maanen et al., 2019). In cognitively demanding tasks, it has been  
238 shown that two distinct components of evidence accumulation (quality and quantity of  
239 evidence) are affected by SAT manipulations, with quantity of evidence being analogous to an  
240 urgency signal (Boag et al., 2019b, 2019a). Recent evidence suggests that different SAT  
241 manipulations can affect different psychological processes: cue-based manipulations that  
242 instruct participants to be fast or accurate, lead to overall threshold adjustments, whereas  
243 deadline-based manipulations lead to a collapse of thresholds (Katsimpokis et al., 2020).

244 Here, we apply an SAT manipulation in an instrumental learning task (Figure 2C). This  
245 paradigm differed from experiment 1 by the inclusion of a cue-based instruction to either stress  
246 response *speed* ('SPD') or response *accuracy* ('ACC') prior to each choice (randomly  
247 interleaved). Furthermore, on speed trials, participants had to respond within 0.7 s to receive a  
248 reward. Feedback was determined based on both the choice's probabilistic outcome ('+100' or  
249 '+0') and the RT: On trials where participants responded too late, they were additionally  
250 informed of the reward associated with their choice, had they been in time, so that they always  
251 received the feedback required to learn from their choices. After exclusions (see methods), data  
252 from 19 participants (324 trials each) were included in the analyses.

253 To illustrate the importance of simultaneously analyzing RTs and choice behavior, we first  
254 test whether a soft-max model (which ignores RTs) is able to capture the behavioral changes  
255 in choice probability due to the manipulation. We fit two soft-max models to the data: One  
256 with a single inverse temperature parameter, and one with an inverse temperature parameter  
257 per SAT condition. The soft-max model with separate parameters per condition was  
258 outperformed by a model with a single parameter ( $\Delta BPIC = 11$ ), indicating that a researcher  
259 using soft-max would have concluded that there was no difference in choice behavior between  
260 conditions. Clearly, the difference in accuracy (and RTs) did indicate there were differences in  
261 behavior (see supplementary materials for formal statistical tests), showing that soft-max fails  
262 to capture a strong and well-known phenomenon of decision-making.

263 Next, we compared the RL-DDM and RL-ARD, and in light of the multiple psychological  
264 mechanisms potentially affected by the SAT manipulation, we allowed different combinations  
265 of threshold, drift rate, and for the RL-ARD urgency, to vary with the SAT manipulation. We  
266 fit three RL-DDM models, varying either threshold, the Q-value weighting on the drift rates  
267 parameter (Sewell and Stallman, 2020), or both. For the RL-ARD, we fit all seven possible  
268 models with different combinations of the threshold, urgency, and drift rate parameters free to  
269 vary between SAT conditions.

270 Formal model comparison (see Supplementary Table S1 for all BPIC values) indicated that  
271 the RL-ARD model combining response caution and urgency effects provides the best  
272 explanation of the data, in line with earlier research in non-learning contexts (Katsimpokis et  
273 al., 2020; Miletic and Van Maanen, 2019; Rae et al., 2014; Thura and Cisek, 2016). The

274 advantage for the RL-ARD was substantial; the best RL-DDM (with only a threshold effect)  
275 performed worse than the worst RL-ARD model. The data and posterior predictive  
276 distributions of the best RL-DDM model and the winning RL-ARD model are shown in Figure  
277 6. As in experiment 1, the RL-DDM failed to capture the shape of RT distributions, although  
278 it fit the SAT effect on accuracy and median RTs. The RL-ARD model provides a much better  
279 account of the RT distributions, including the differences between SAT conditions. In  
280 supplementary materials we show that adding non-decision time variability to the RL-DDM  
281 mitigates some of the misfit of the RT distributions, although it still consistently under-  
282 predicted the 10<sup>th</sup> percentile in the accuracy condition. Further, this model was still  
283 substantially outperformed by the RL-ARD in formal model selection ( $\Delta\text{BPIC} = 209$ ), and non-  
284 decision time variability was estimated as much greater than what is found in non-learning  
285 context, raising the question of its psychological plausibility.

286 Both RL-DDM and RL-ARD models tended to underestimate RTs and choice accuracy in  
287 the early trial bins in the accuracy emphasis condition. As in experiment 1, working memory  
288 may have contributed to the accurate but slow responses in the first trial bin for the accuracy  
289 condition (Collins and Frank, 2018, 2012b; McDougle and Collins, 2020).

290

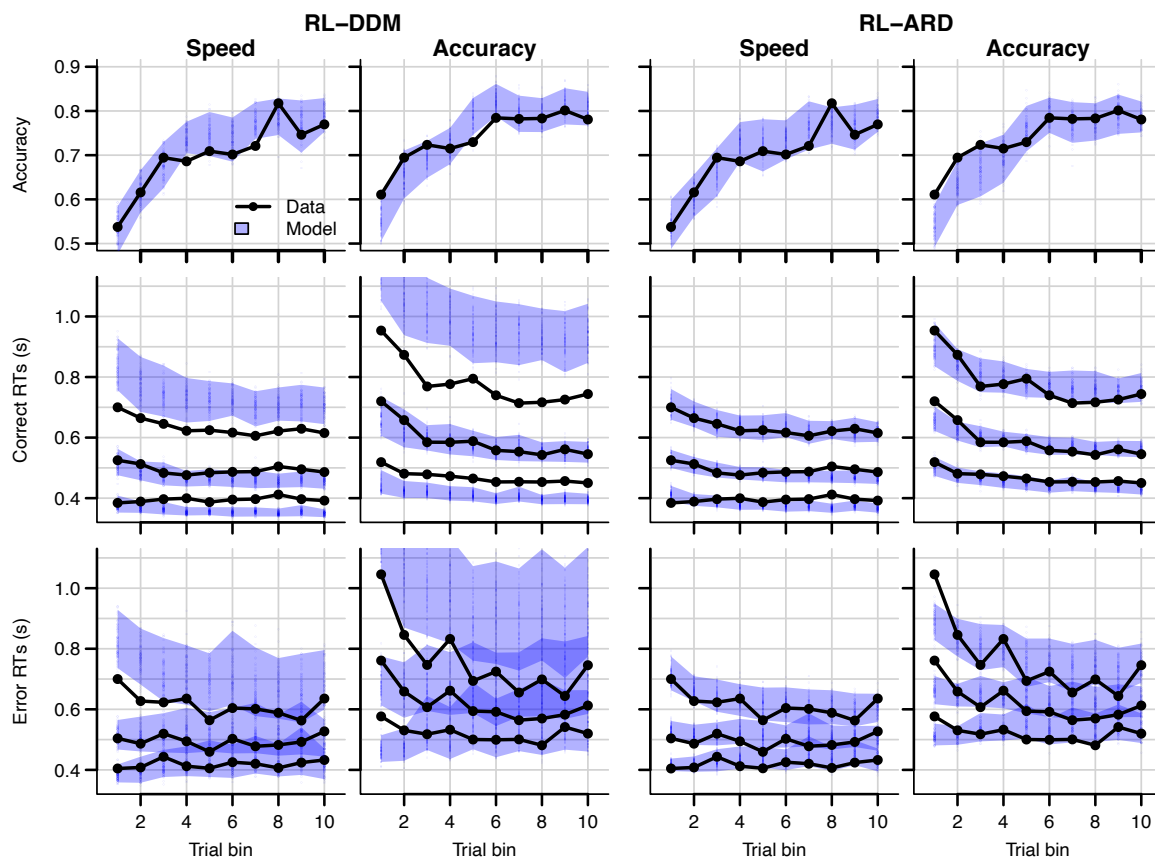


Figure 6. Data (black) and posterior predictive distributions (blue) of the best-fitting RL-DDM (left columns) and the winning RL-ARD model (right columns), separate for the speed and accuracy emphasis conditions. Top row depicts accuracy over trial bins. Middle and bottom row show 10<sup>th</sup>, 50<sup>th</sup>, and 90<sup>th</sup> RT percentiles for the correct (middle row) and error (bottom row) response over trial bins. Shaded areas in the middle and right column correspond to the 95% credible interval of the posterior predictive distribution.

291

## 292 **Reversal learning**

293 Finally, we tested whether the RL-ARD can capture changes in accuracy and RTs caused by a  
294 perturbation in the learning process due to reversals in reward contingencies. In the reversal  
295 learning paradigm (Behrens et al., 2007; Costa et al., 2015; Izquierdo et al., 2017) participants  
296 first learn a contingency between choice options and probabilistic rewards (the acquisition  
297 phase) that is then suddenly reversed without any warning (the reversal phase). If the link  
298 between Q-values and decision mechanisms as proposed by the RL-ARD underlies decisions,  
299 the model should be able to account for the behavioral consequences (RT distributions and  
300 decisions) of Q-value changes induced by the reversal.

301 Our reversal learning task had the same general structure as experiment 1 (Figure 1), except  
302 for the presence of reversals. 47 participants completed four blocks of 128 trials each. Within  
303 each block, two pairs of stimuli were randomly interleaved. Between trials 61 and 68  
304 (uniformly sampled) in each block, the reward probability switched between stimuli, such that  
305 stimuli that were correct during acquisition were incorrect after reversal (and vice versa).  
306 Participants were not informed of the reversals prior to the experiment, but many reported  
307 noticing them.

308 Data and the posterior predictive distributions of the RL-DDM and the RL-ARD models are  
309 shown in Figure 7. Both models captured the change in choice proportions after the reversal  
310 reasonably well, although they underestimate the speed of change. In supplementary materials  
311 we show that the same is true for a standard soft-max model, suggesting that the learning rule  
312 is the cause of this problem. Recent evidence indicates that, instead of only estimating expected  
313 values of both choice options by error-driven learning, participants may additionally learn the  
314 task structure, estimate the probability of a reversal occurring and adjust choice behavior  
315 accordingly. Such a model-based learning strategy could increase the speed with which choice  
316 behavior changes after a reversal (Costa et al., 2015; Izquierdo et al., 2017; Jang et al., 2015),  
317 but as yet a learning rule that implements this strategy has not been developed.

318 The change in RT around the reversal was less marked than the change in choice probability.  
319 Once again, the RL-DDM overestimates variability and skew. Both models fit the effects of  
320 learning and reversal similarly, but the fastest responses for the RL-DDM decrease much too  
321 quickly during initial learning and the reduction in speed for the slowest responses due to the  
322 reversal is strongly overestimated. The RL-ARD provides a much better account of the shape  
323 of the RT distributions, and furthermore captures the increase in entire RT *distributions*  
324 (instead of only the median) after the reversal point. Formal model comparison also very  
325 strongly favors the RL-ARD over the RL-DDM ( $\Delta BPIC = 4051$ ). Supplementary materials  
326 provide model comparisons to RL-DDMs with between-trial variability parameters, which lead  
327 to the same conclusion.

328 A notable aspect of the data is that choice behavior stabilizes approximately 20 trials after  
329 the reversal, whereas RTs remain high compared to just prior to the reversal point for up to ~40  
330 trials. The RL-ARD explains this behavior through relatively high Q-values for the choice  
331 option that was correct during the acquisition (but not reversal) phase (i.e., choice A). Figure  
332 8 depicts the evolution of Q-values, Q-value differences and sums, and drift rates in the RL-  
333 ARD model. The Q-values for both choice options increase until the reversal (Figure 8A), with  
334 a much faster increase for  $Q_A$ . At the reversal  $Q_A$  decreases and  $Q_B$  increases, but as  $Q_A$

335 decreases faster than  $Q_B$  increases there is a temporary decrease in Q-value sums (Figure 8C).  
 336 After approximately 10 trials post-reversal,  $Q_B$  is higher than for  $Q_A$ , which flips the sign of  
 337 the Q-value differences (Figure 8B). However,  $Q_A$  after the reversal remains higher than the  
 338  $Q_B$  before the reversal, which causes the (absolute) Q-value differences to be lower after the  
 339 reversal than before. As a consequence, the drift rates for B after the reversal remain lower than  
 340 the drift rates for A before the reversal, which increases RT. Clearly, it is important to take  
 341 account of the sum of inputs to accumulators as well as the difference between them in order  
 342 to provide an accurate account of the effects of learning.  
 343

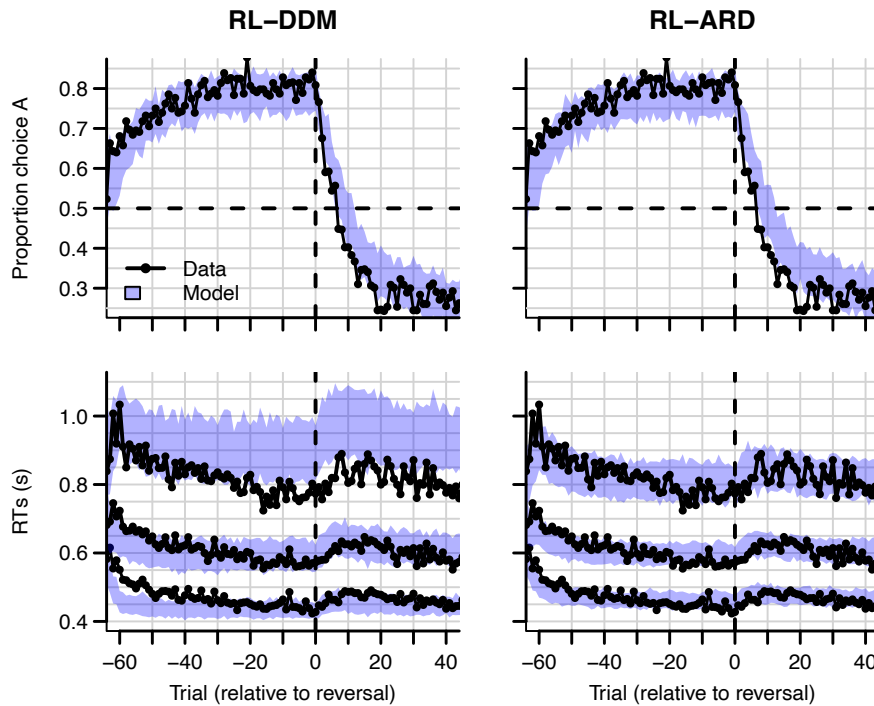


Figure 7. Experiment 3 data (black) and posterior predictive distributions (blue) for the RL-DDM (left) and RL-ARD (right). Top row: choice proportions over trials, with choice option A defined as the high-probability choice before the reversal in reward contingencies. Bottom row: 10<sup>th</sup>, 50<sup>th</sup>, and 90<sup>th</sup> RT percentiles. The data are ordered relative to the trial at which the reversal first occurred (trial 0, with negative trial numbers indicated trials prior to the reversal). Shaded areas correspond to the 95% credible interval of the posterior predictive distributions.

344

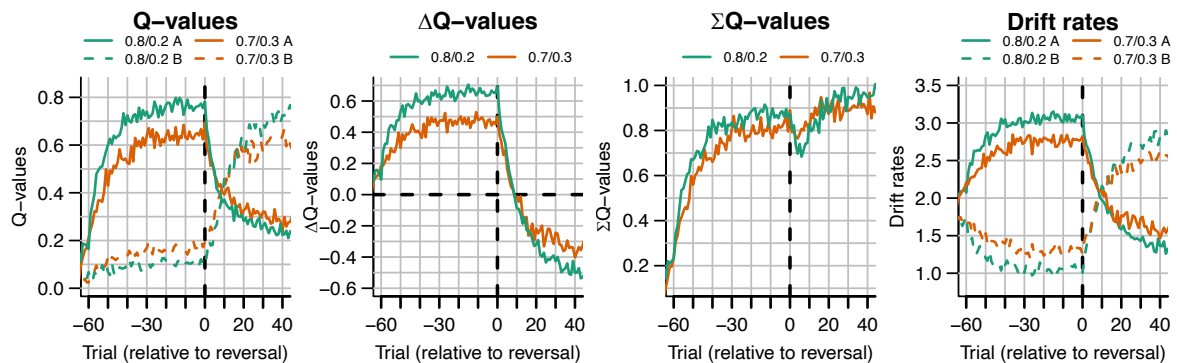


Figure 8. The evolution of Q-values and their effect on drift rates in the RL-ARD in experiment 3, aggregated across participants. Left panel depicts raw Q-values, separate for each difficulty condition (colors). The second and third panel depict the Q-value differences and the Q-value sums over time. The drift rates (right panel) are a weighted sum of the Q-value differences and Q-value sums, plus an intercept. Choice A (solid lines) refers to the option that had the high probability of reward during the acquisition phase, and choice B (dashed lines) to the option that had the high probability of reward after the reversal.

345

346

## 347 Discussion

348 We compared combinations of different evidence-accumulations models with a simple SARSA  
349 (Rummery and Niranjan, 1994) reinforcement learning rule (RL-EAMs). The comparison  
350 tested the ability of the RL-EAMs to provide a comprehensive account of behavior in learning  
351 contexts, not only in terms of the choices made but also the full distribution of the times to  
352 make them (RT). We examined a standard instrumental learning paradigm (Frank, 2004) that  
353 manipulated the difference in rewards between binary options (i.e., decision difficulty). We  
354 also examined two elaborations of that paradigm testing key phenomena from the decision-  
355 making and learning literatures, speed-accuracy trade-offs (SAT), and reward reversals,  
356 respectively. Our benchmark was the dual threshold Diffusion Decision Model (Ratcliff, 1978)  
357 (DDM), which has been used in almost all previous RL-EAM research, but has not been  
358 compared to other RL-EAMs, and has not been thoroughly evaluated on its ability to account  
359 for RT distributions in learning tasks. Our comparison used several different racing diffusion  
360 (RD) models, where decisions depend on the winner of a race between single barrier diffusion  
361 processes.

362 The RL-DDM provided a markedly inferior account to the other models, consistently  
363 overestimating RT variability and skew. As these aspects of behavior are considered critical in  
364 evaluating models in decision-making literature (Forstmann et al., 2016; Ratcliff and McKoon,  
365 2008; Voss et al., 2013), our results question whether the RL-DDM provides an adequate  
366 model of instrumental learning. Furthermore, the DDM carries with it two important theoretical  
367 limitations. First, it can only address binary choice. This is unfortunate given that perhaps the  
368 most widely used clinical application of reinforcement learning, the Iowa gambling task  
369 (Bechara et al., 1994), requires choices among four options. Second, the input to the DDM  
370 combines the evidence for each choice (i.e., “Q” values determined by the learning rule) into a  
371 single difference, and so requires extra mechanisms to account for known effects of overall  
372 reward magnitude (Fontanesi et al., 2019a). Although there are potential ways that the RL-  
373 DDM might be modified to account for magnitude effects, such as increasing between-trial  
374 drift rate variability in proportion to the mean rate (Ratcliff et al., 2018), its inability to extend  
375 beyond binary choice remains an enduring impediment.

376 The best alternative model that we tested, the RL-ARD (advantage racing diffusion), which  
377 is based on the recently proposed advantage accumulation framework (Van Ravenzwaaij et al.,  
378 2020), remedied all of these problems. The input to each accumulator is the weighted sum of  
379 three components: stimulus independent “urgency”, the difference between evidence for the  
380 choice corresponding to the accumulator and the alternative (the advantage), and the sum of  
381 the evidence over accumulators. The urgency component had large effect in all fits and played

382 a key role in explaining the effect of speed-accuracy trade-offs. The advantage component,  
383 which is similar to the input to the DDM, was strongly supported over a model in which each  
384 accumulator only receives evidence favoring its own choice. The sum component provided a  
385 simple and theoretically transparent way to deal with reward magnitude effects in instrumental  
386 learning. Despite having the weakest effect among the three components, the sum was clearly  
387 necessary to provide an accurate fit to our data, even though we did not manipulate reward  
388 magnitude. It also played an important role in explaining the effect of reward reversals.

389 It is perhaps surprising that the RL-DDM consistently overestimated RT variability and  
390 skewness given that the DDM typically provides much better fits to data from perceptual  
391 decision-making tasks without learning. The inclusion of between-trial variability in non-  
392 decision times partially mitigated the misfit but required an implausibly high non-decision time  
393 variability, and model comparisons still favored the RL-ARD. Previous work on the RL-DDM  
394 did not investigate this issue. In many RL-DDM papers, RT distributions are either not  
395 visualized at all, or are plotted using (defective) probability density functions on top of a  
396 histogram of RT data, making it hard to detect misfit, particularly with respect skew due to the  
397 slow tail of the distribution. One exception is Pedersen et al. (2020), whose quantile-based  
398 plots show the same pattern that we found here of over-estimated variability and skewness for  
399 more difficult choice conditions, despite including between-trial variability in non-decision  
400 times. In a non-learning context, it has been shown that the DDM overestimates skewness in  
401 high-risk preferential choice data (Dutilh and Rieskamp, 2016). Together these results suggest  
402 that decision processes in value-based decision in general, and instrumental learning tasks in  
403 particular, may be fundamentally different from a two-sided diffusion process, and instead  
404 better captured by a race model such as the RL-ARD.

405 In the current work, we chose to use racing diffusion processes over the more often used  
406 LBA models for reasons of parsimony: error-driven learning introduces between-trial  
407 variability in accumulation rates, which are explicitly modelled in the RL-EAM framework.  
408 As the LBA includes between-trial variability in drift rates as a free parameter, multiple  
409 parameters can account for the same variance. Nonetheless, exploratory fits (see the  
410 supplementary materials) confirmed our expectation that an RL-ALBA (Advantage ALBA)  
411 model fit the data of experiment 1 well, although formal model comparisons preferred the RL-  
412 ARD. Future work might consider completely replacing one or more sources of between trial  
413 variability in the LBA with structured fluctuations due to learning and adaption mechanisms.

414 The parametrization of the ARD model used in the current paper followed van Ravenzwaaij  
415 et al.'s (2020) proposed ALBA model. This parametrization interprets the influence on drift  
416 rates in terms of advantages and magnitudes. However, as both the weights on Q-value  
417 differences and sums ( $w_D$  and  $w_S$ ) are freely estimated parameters, the equations that define  
418 the drift rates can be rearranged as follows:

419

$$\begin{aligned} dx_1 &= [V_0 + w_e Q_1 - w_i Q_2]dt + sW \\ dx_2 &= [V_0 + w_e Q_2 - w_i Q_1]dt + sW \end{aligned} \quad (5)$$

420

421 Where  $w_e$  equals the sum of  $w_D$  and  $w_S$  in the parametrization of Equation (4), and  $w_i$  equals  
422 the difference between  $w_D$  and  $w_S$ . This re-parametrization shows that each drift rate is  
423 determined by an excitatory influence  $w_e$  of the Q-value associated with the accumulator, and



424 an inhibitory influence  $w_i$  of the Q-value associated with the other accumulator. Turner (2019)  
425 proposed that inhibition plays an important role in learning tasks. Although the locus of  
426 inhibition is different in the two models, there are clear parallels that bear further investigation.

427 A limitation of the current work is that we collapsed across blocks in analyzing the data of  
428 experiments 2 and 3. However, in more detailed explorations (see supplementary materials for  
429 details) there were indications of second-order changes across blocks. In experiment 2,  
430 participants were faster in the first trial bin of the second and third block compared to the first  
431 block, suggesting additional practice or adaptation effects at the beginning of the experiment.  
432 In experiment 3, participants slowed down, and learned the reversal faster, after the first block.  
433 This suggests they learned about the presence of reversals in the first block and applied a  
434 different strategy in the later blocks. Although it is known that participants increase their  
435 learning rates in volatile environments (Behrens et al., 2007), this by itself does not explain a  
436 decrease in response speed. Potentially, if participants understood the task structure after the  
437 first block, model-based strategies, such as estimating the probability of a reversal having  
438 occurred, also slowed down responses.

439 Although the account of data provided by the RL-ARD model was generally quite accurate,  
440 some elements of misfit suggest the need for further model development. RT and accuracy  
441 were underestimated in the initial trials of the easiest condition in experiment 1, in the accuracy  
442 emphasis condition in experiment 2, and prior to reversals in experiment 3. Furthermore, the  
443 RL-ARD model underestimated the speed with which choice probability changed after reversal  
444 of stimulus-response mappings. These misfits point to a limited ability to capture the learning-  
445 related changes in behavior. This is to some degree unsurprising, since we used a very simple  
446 model of error-driven learning. Future work might explore more sophisticated mechanisms,  
447 such as multiple learning rates (Daw et al., 2002; Fontanesi et al., 2019a; Gershman, 2015;  
448 Pedersen et al., 2017) or different learning rules (Fontanesi et al., 2019b, 2019a). Furthermore,  
449 there is clearly a role for working memory in some reinforcement learning tasks (Collins and  
450 Frank, 2018, 2012b), likely explaining the accurate but slow responses we observed in the early  
451 trial bins for easy conditions.

452 In summary, we believe that the ARD decision mechanism provides a firm basis for further  
453 explorations of the mutual benefits that arise from the combination of reinforcement learning  
454 and evidence-accumulation models, providing constraint that is based on a more  
455 comprehensive account of data than has been possible in the past. As it stands, the RL-ARD's  
456 parameter recovery properties are good even with relatively low trial numbers, making it a  
457 suitable measurement model for simultaneously studying learning and decision-making  
458 processes, and inter-individual differences therein. Further, the advantage framework extends  
459 to multiple choice while maintaining analytical tractability and addressing key empirical  
460 phenomena in that domain, such as Hick's Law and response-competition effects (Van  
461 Ravenzwaaij et al., 2020), enabling future applications to clinical settings, such as in the Iowa  
462 gambling task (Bechara et al., 1994).

463

## 464 **Methods**

### 465 **Experiment 1**

#### 466 *Participants*

467 61 participants (mean age 21y [SD 2.33], 47 women, 56 right handed) were recruited from the  
468 subject pool of the department of Psychology, University of Amsterdam, and participated for  
469 course credits. All participants had normal or corrected-to-normal vision and gave written  
470 informed consent prior to the experiment onset. The study was approved by the local ethics  
471 committee.

472

### 473 *2.1.2 Task*

474 The task was an instrumental probabilistic learning task (Frank, 2004). On each trial, the  
475 subject was presented with two abstract symbols (a ‘stimulus pair’) representing two choice  
476 options (see Figure 2A for an example trial). Each choice option had a fixed probability of  
477 being rewarded with points when chosen, with one choice option always having a higher  
478 probability of being rewarded than the other. The task is to discover, by trial and error, which  
479 choice options are most likely to lead to rewards, and thereby to collect as many points as  
480 possible.

481 After a short practice block to get familiar with the task, participants completed one block  
482 of 208 trials. Four different pairs of abstract symbols were included, each presented 52 times.  
483 Stimulus pairs differed in their associated reward probabilities: 0.8/0.2, 0.7/0.3, 0.65/0.35, and  
484 0.6/0.4. The size of the reward, if obtained, was always the same: ‘+100’ (or ‘+0’ otherwise).  
485 Reward probabilities were chosen such that they differed only in the between-choice difference  
486 in reward probability, leading to varying choice difficulties while keeping the mean reward  
487 magnitude fixed.

488 Participants were instructed to earn as many points as possible, and to always respond before  
489 the deadline of 2 seconds. Feedback consisted of two parts: an ‘outcome’ and a ‘reward’. The  
490 outcome corresponded to the probabilistic outcome of the choice, whereas the reward  
491 corresponded to the actual number of earned points. When participants responded before the  
492 deadline, the reward was equal to the outcome. If they were too late, the outcome was shown  
493 to allow participants to learn from their choice, but the reward they received was set to 0 to  
494 encourage responding in time. Participants received a bonus depending on the number of points  
495 earned (maximum +0.5 course credits, mean received +0.24). The task was coded in PsychoPy  
496 (Peirce et al., 2019). After this block, participants performed two more blocks of the same task  
497 with different manipulations, which are not of current interest.

498

### 499 *Exclusion*

500 Six participants were excluded from analysis: One reported, after the experiment, not to have  
501 understood the task, one reported a technical issue, and four did not reach an above-chance  
502 accuracy level as determined by a binomial test (accuracy cut-off 0.55, corresponding to  
503  $p < 0.05$ ). The final sample thus consisted of 55 subjects (14 men, mean age 21 years old [SD  
504 2.39], 51 right-handed).

505

### 506 *Cognitive modelling*

507 The main analysis consists of fitting four RL-EAMs to the data and comparing the quality of  
508 the fits penalized by model complexity. We compared four different decision models: the DDM  
509 (Ratcliff, 1978), a racing diffusion (Boucher et al., 2007; Logan et al., 2014; Purcell et al.,  
510 2010; Turner, 2019) model, and two Advantage Racing Diffusion (ARD; Van Ravenzwaaij et

511 al., 2020) models (see Figure 1 for an overview). Whereas the former is a two-sided diffusion  
512 process, the latter three models employ a race architecture.

513 For all models we used the State-Action-Reward-State-Action (SARSA; Rummery and  
514 Niranjana, 1994) update rule as a learning model:

515

$$Q_{i,t+1} = Q_{i,t} + \alpha(r_t - Q_{i,t}) \quad (4)$$

516

517 where  $Q_{i,t}$  is the value representation of choice option  $i$  on trial  $t$ ,  $\alpha$  the learning rate, and  $r_t$   
518 the reward on trial  $t$ . The difference between the actual reward and the value representation of  
519 the chosen stimulus,  $r_t - Q_{i,t}$ , is known as the reward prediction error. The learning rate  
520 controls the speed at which Q-values change in response to the reward prediction error, with  
521 larger learning rates leading to stronger fluctuations. In this model, only the Q-value of the  
522 chosen option is updated.

523

#### 524 *RL-EAM 1: RL-DDM*

525 In the first RL-EAM, we use the DDM (Ratcliff, 1978) as a choice model (Figure 1, left  
526 column). The DDM assumes that evidence accumulation is governed by:

527

$$dx = vdt + sW$$

528

529  $v$  is the mean speed of evidence accumulation (the *drift rate*), and  $s$  is the standard deviation  
530 of the within-trial accumulation white noise (W). The RL-DDM assumes that the drift rate  
531 depends linearly on the difference of value representations:

532

$$v_t = w(Q_{t,1} - Q_{t,2})$$

533

534  $w$  is a weighting variable, and  $Q_{t,1}$  and  $Q_{t,2}$  are the Q-values for both choice options per trial,  
535 which change each trial according to Equation 4. Hence,

536

$$dx = w(Q_1 - Q_2) dt + sW \quad (1)$$

537

538 The starting point of evidence accumulation,  $z$ , lies between decision boundaries  $a$  and  $-a$ .  
539 Here, as in earlier RL-DDM work (Fontanesi et al., 2019a, 2019b; Pedersen et al., 2017), we  
540 assume an unbiased start of the decision process (i.e.,  $z = 0$ ). Evidence accumulation finishes  
541 when threshold  $a$  or  $-a$  is reached, and the decision for the choice corresponding to  $Q_1$  or  $Q_2$ ,  
542 respectively, is made. The response time is the time required for the evidence-accumulation  
543 process to reach the bound, plus an intercept called the non-decision time ( $t_0$ ). The non-  
544 decision time is the sum of the time required for perceptual encoding and the time required for  
545 the execution of the motor response. Parameter  $s$  was fixed to 1 to satisfy scaling constraints  
546 (Donkin et al., 2009; van Maanen and Miletic, 2020). In total, this specification of the RL-  
547 DDM has 4 free parameters ( $\alpha, w, a, t_0$ ). In the supplementary materials, we fit an RL-DDM  
548 specification with between-trial variabilities in start point, drift rate, and non-decision time.

549

550 *RL-EAM 2: RL-RD*

551 The RL-RD (Figure 1, middle panel) assumes that two evidence accumulators independently  
552 accrue evidence for one choice option each, both racing towards a common threshold  $a$   
553 (assuming no response bias). The first accumulator to hit the bound wins, and the  
554 corresponding decision is made. For each choice option  $i$ , the dynamics of accumulation are  
555 governed by:

556

$$dx_i = [V_0 + wQ_i]dt + sW \quad (2)$$

557

558  $V_0$  is a parameter specifying the drift rate in the absence of any evidence,  $w$  a weighting  
559 parameter, and  $s$  the standard deviation of within-trial noise. As such, the mean speed of  
560 accumulation (the drift rate  $v_i$ ) is the sum of two independent factors: an evidence-independent  
561 baseline speed  $V_0$ , and an evidence-dependent weighted Q-value,  $wQ_i$ . Since  $V_0$  is assumed to  
562 be identical across accumulators, and governs the speed of accumulation unrelated to the  
563 amount of evidence, we interpret this parameter as an additive urgency signal (Miletić and Van  
564 Maanen, 2019), with conceptually similar behavioral effects as collapsing bounds (Hawkins et  
565 al., 2015). Similar to the DDM, a non-decision time parameter accounts for the time for  
566 perceptual encoding and the motor response time. Parameter  $s$  was fixed to 1 to satisfy scaling  
567 constraints (Donkin et al., 2009; van Maanen and Miletić, 2020). In total, the RL-RD has 5 free  
568 parameters ( $\alpha, w, a, v_0, t_0$ ).

569 Each accumulator's first passage times are Wald (also known as inverted Gaussian)  
570 distributed (Anders et al., 2016). In an independent race model, each accumulator's first  
571 passage time distribution is normalized to the probability of the response with which it is  
572 associated (Brown and Heathcote, 2008; Turner, 2019).

573

574 *RL-EAM 3 & 4: RL-ARD*

575 Thirdly, we fit two racing diffusion models based on an advantage race architecture (Van  
576 Ravenzwaaij et al., 2020). An advantage race model using an LBA has been shown to provide  
577 a natural account for multi-alternative choice phenomena such as Hick's law, as well as  
578 stimulus magnitude effects in perceptual decision-making. Like in the RL-RD, accumulators  
579 race towards a common bound, but the speed of evidence accumulation  $v_i$  depends on multiple  
580 factors: first, as in the RL-RD, the evidence-independent speed of accumulation  $V_0$ ; second,  
581 the *advantage* of the evidence for one choice option over the other (c.f. the DDM, where the  
582 difference between evidence for both choice options is accumulated); and third, the *sum* of the  
583 total available evidence. Combined, for two accumulators in the RL-EAM framework, this  
584 leads to:

585

$$\begin{aligned} dx_1 &= [V_0 + w_a(Q_1 - Q_2) + w_s(Q_1 + Q_2)]dt + sW \\ dx_2 &= [V_0 + w_a(Q_2 - Q_1) + w_s(Q_1 + Q_2)]dt + sW \end{aligned} \quad (3)$$

586

587 In the original work proposing the advantage accumulation framework (Van Ravenzwaaij et  
588 al., 2020), it was shown that the  $w_a$  parameter had a much stronger influence on evidence-

589 accumulation rates than the  $w_s$  parameter. Therefore, we first fixed the  $w_s$  parameter to 0, to  
590 test whether the accumulation of *differences* is sufficient to capture all trends in the data. We  
591 term this model the RL-lARD (l = limited), which we compare to the RL-ARD in which we fit  
592  $w_s$  as a free parameter.

593 As previously, parameter  $s$  was fixed to 1 to satisfy scaling constraints (Donkin et al., 2009;  
594 van Maanen and Miletić, 2020). The RL-ARD also has a threshold, non-decision time, and  
595 learning rate parameter, totaling five ( $\alpha, w_d, a, V_0, t_0$ ) and 6 free parameters  
596 ( $\alpha, w_d, w_s, a, V_0, t_0$ ) for the RL-lARD and RL-ARD, respectively.

597

598 *Bayesian hierarchical parameter estimation, posterior predictive distributions, model*  
599 *comparisons*

600 We estimated group-level and subject-level posterior distributions of each model's parameter  
601 using a combination of differential evolution (DE) and Markov-chain Monte Carlo sampling  
602 (MCMC) with Metropolis-Hastings (Ter Braak, 2006; Turner et al., 2013). Sampling settings  
603 were default as implemented in the Dynamic Models of Choice *R* software (Heathcote et al.,  
604 2019): The number of chains,  $D$ , was three times the number of free parameters. Cross-over  
605 probability was set to  $2.38/\sqrt{D}$  at the subject-level and  $U[0, 1]$  at the group level. Migration  
606 probability was set to 0.05 during burn-in only. Convergence was assessed using visual  
607 inspection of the chain traces and Gelman-Rubin diagnostic (Brooks and Gelman, 1998;  
608 Gelman and Rubin, 1992) (individual and multivariate potential scale factors  $< 1.03$  in all  
609 cases).

610 Hierarchical models were fit assuming independent normal population (“hyper”)   
611 distributions for each parameter. For all models, we estimated the learning rate on a probit scale  
612 (mapping  $[0, 1]$  onto the real domain), with a normal prior  $\alpha \sim \Phi(\mathcal{N}(-1.6, 5))$  (Spektor and  
613 Kellen, 2018). Prior distributions for all estimated hyper-mean decision-related parameters  
614 were vague. RL-EAMs, the threshold parameter  $a \sim \mathcal{N}(3, 5)$  truncated at 0, and  
615  $t_0 \sim \mathcal{N}(0.3, 0.5)$  truncated at 0.025 s and 1 s (all estimation was carried out on the seconds  
616 scale). For the RL-DDM,  $w \sim \mathcal{N}(2, 5)$ . For the RL-RD,  $w \sim \mathcal{N}(9, 5)$ , and for the RL-ARD  
617 models,  $w_D \sim \mathcal{N}(9, 5)$  and  $w_s \sim \mathcal{N}(0, 3)$ . For the hyper-SD, a  $\Gamma(1,1)$  distribution was used  
618 as prior. Plots of superimposed prior and posterior hyper-distributions confirmed that these  
619 prior setting were not influential.

620 In initial explorations, we also freely estimated the Q-values at trial 0. However, in the RL-  
621 EAMs, the posterior distributions for these Q-values consistently converged on 0, which was  
622 therefore subsequently used as a fixed value for all results reported here. For the the soft-max  
623 fits, they were set to 0.5 as often used in reinforcement learning models of two-choice tasks  
624 (Apps et al., 2015; Collins and Frank, 2018, 2012b; Fontanesi et al., 2019a; McDougle and  
625 Collins, 2020; Pedersen and Frank, 2020). Including the initial Q-values as a free parameter in  
626 the soft-max models of experiment 2 led to the same conclusions.

627 To visualize the quality of model fit, we took 100 random samples from the estimated  
628 parameter posteriors and simulated the experimental design with these parameters. For each  
629 behavioral measure (e.g., RT quantiles, accuracy), credible intervals were estimated by taking  
630 the range between the 2.5% and 97.5% quantiles of the averages over participants.

631 To quantitatively compare the fit of different models, penalized by their complexity, we  
632 used the Bayesian predictive information criterion (BPIC; Ando, 2007). The BPIC is an  
633 analogue of the Bayesian information criterion (BIC), but (unlike the BIC) suitable for models  
634 estimated using Bayesian methods. Compared to the deviance information criterion (DIC;  
635 Spiegelhalter et al., 2002), the BPIC penalizes model complexity more strongly to prevent  
636 over-fitting (c.f. AIC vs. BIC). Lower BPIC values indicate better trade-offs between fit quality  
637 and model complexity.

638

## 639 **Experiment 2**

### 640 *Participants*

641 23 participants (mean age 19 years old [SD 1.06 years], 7 men, 23 right-handed) were recruited  
642 from the subject pool of the Department of Psychology of the University of Amsterdam and  
643 participated for course credits. Participants did not participate in experiment 1 or 3. All  
644 participants had normal or corrected-to-normal vision and gave written informed consent prior  
645 to the experiment onset. The study was approved by the local ethics committee.

646

### 647 *Task*

648 Participants performed the same task as in experiment 1, with the addition of an SAT  
649 manipulation (Figure 2C). The SAT manipulation included both an instructional cue and a  
650 response deadline. Prior to each trial, a cue instructed participants to emphasize either decision  
651 speed ('SPD') or decision accuracy ('ACC') in the upcoming trial, and in speed trials,  
652 participants did not earn points if they were too late ( $> 700$  ms). As in experiment 1, after each  
653 choice participants received feedback consisting of two components: an outcome and a reward.  
654 The outcome refers to the outcome of the probabilistic gamble, whereas the reward refers to  
655 the number of points participants actually received. If participants responded in time, the  
656 reward was equal to the outcome. In speed trials, participants did not earn points if they  
657 responded later than 700 ms after stimulus onset, even if the outcome was +100. On trials  
658 where participants responded too late, they were additionally informed of the reward that was  
659 associated with their choice, had they been in time. This way, even when participants are too  
660 late, they still receive the feedback that can be used to learn from their choices.

661 The deadline manipulation was added because we hypothesized that instructional cues alone  
662 would not be sufficient to persuade participants to change their behavior in the instrumental  
663 learning task, since that task specifically requires them to accumulate points. If the received  
664 number of points was independent of response times, the optimal strategy to collect most points  
665 would be to ignore the cue and focus on accuracy only.

666 Participants performed 324 trials divided over 3 blocks. Within each block, three pairs of  
667 stimuli were shown, with associated reward probabilities of 0.8/0.2, 0.7/0.3, and 0.6/0.4. Speed  
668 and accuracy trials were randomly interleaved. Figure 2C depicts the sequence of events in  
669 each trial. As this experiment also served as a pilot for an fMRI experiment, we added fixation  
670 crosses between each phase of the trial, with jittered durations. A pre-stimulus fixation cross  
671 lasted 0.5, 1, 1.5, or 2 s; fixation crosses between cue and stimulus, between stimulus and  
672 highlight, and between highlight and feedback lasted 0, 0.5, 1, or 1.5 s; and an inter-trial  
673 interval fixation cross lasted 0.5, 1, 1.5, 2, 2.5 seconds. Each trial took 7.5 seconds. The  
674 experiment took approximately 45 minutes.

675

### 676 *Exclusion*

677 Four participants did not reach above-chance performance as indicated by a binomial test (cut-  
678 off 0.55,  $p < 0.05$ ), and were excluded from further analyses. The final sample thus consisted  
679 on 19 participants (mean age 19 years old [SD 1.16 years], 6 men, 19 right-handed). For one  
680 additional participant, a technical error occurred after the first block. This participant was  
681 included in the analyses, since the Bayesian estimation framework naturally down-weights the  
682 influence of participants with fewer trials.

683

### 684 *Cognitive modelling*

685 First, we tested whether a standard soft-max model is able to capture the difference in choice  
686 behavior. Soft-max is given by:

687

$$P_{i,t} = \frac{\exp \beta Q_{i,t}}{\sum_j \exp \beta Q_{j,t}} \quad (5)$$

688

689 where  $P_{i,t}$  is the probability of choosing option  $i$  on trial  $t$ ,  $J$  is the total number of choice  
690 options, and  $\beta$  is a free parameter often called the inverse temperature. The inverse temperature  
691 is often interpreted in terms of the exploration/exploitation trade-off (Daw et al., 2006), with  
692 higher values indicating more exploitation. In two-choice settings, Equation 5 can be re-written  
693 as:

694

$$P_{2,t} = \frac{1}{1 + \exp \beta (Q_{1,t} - Q_{2,t})} \quad (6)$$

695

696 which highlights that the choice probability is driven by the *difference* in Q-values, weighted  
697 by the inverse temperature parameter. We hierarchically fit two soft-max models using the  
698 same parameter estimation methods as in experiment 1. One model assumed a single  $\beta$   
699 parameter, the other model assumed a  $\beta$  parameter per SAT condition. Priors for the hypermean  
700 were set to  $\beta \sim N(1,5)$  truncated at 0, and for the hyperSD  $\Gamma(1,1)$ .

701 Next, we fit three RL-DDMs and seven RL-ARDs. The three RL-DDM models varied either  
702 threshold, the Q-value weighting on the drift rates parameter (Sewell and Stallman, 2020), or  
703 both. The seven RL-ARD allowed all unique combinations of the threshold, urgency, and drift  
704 rate parameters free to vary between the speed and accuracy conditions.

705 For the accuracy condition, we used the same priors as in experiment 1. In the speed  
706 condition, the parameters that were free to vary were estimated as proportional differences  
707 from the accuracy conditions; specifically:  $a_{spd} = (1 + m_{a,spd}) * a_{acc}$ ,  $V_{0,spd} = (1 +$   
708  $m_{V_0,spd}) * V_{0,acc}$ , and  $v_{i,spd} = (1 + m_{v,spd}) * v_{i,acc}$ . The prior used was  $\mathcal{N}(0,5)$  for the  
709 hypermean and  $\Gamma(1,1)$  for the hyperSD of all parameters  $m$ , truncated at -1.

710

## 711 **Experiment 3**

### 712 *Participants*

713 47 participants (mean age 21 years old [SD 2.81 years], 16 men, 40 right-handed) were  
714 recruited from the subject pool of the Department of Psychology of the University of  
715 Amsterdam and participated for course credits. Participants did not participate in experiment 1  
716 or 2. All participants had normal or corrected-to-normal vision and gave written informed  
717 consent prior to the experiment onset. The study was approved by the local ethics committee.

718

#### 719 *Task*

720 The reversal learning task had the same general task structure as experiment 1. Participants  
721 completed four blocks of 128 trials each, totaling 512 trials. Within each block, two pairs of  
722 stimuli were randomly interleaved, with associated reward probabilities of 0.8/0.2 and 0.7/0.3.  
723 Between trials 61 and 68 (uniformly sampled) of each block, the reward probability switched  
724 between stimuli, such that the stimulus with a pre-reversal reward probability of 0.8/0.7 had a  
725 post-reversal reward probability of 0.2/0.3 (and vice versa). Participants were not informed of  
726 the reversals prior to the experiment, but many reported noticing them.

727 In addition to the reversal learning task, the experimental session also contained a working  
728 memory task that is not of current interest. 30 participants performed the reversal learning task  
729 before the working memory task, and 17 participants afterwards. The entire experiment took  
730 approximately one hour.

731

#### 732 *Cognitive modelling*

733 The RL-DDM and RL-ARD were fit to the data using the same methods as in experiment 1.

734

735

#### 736 **Data availability statement**

737 All data are available on OSF (<https://osf.io/ygrve/>).

738

#### 739 **Code availability statement**

740 All analysis code is available on OSF (<https://osf.io/ygrve/>).

741

#### 742 **Acknowledgements**

743 We thank Barbara Mathiopoulou and Chris Riddell for their help collecting the data. This work  
744 was supported by an NWO-VICI grant (BUF), an ABC VIP grant and ARC DP150100272 and  
745 DP160101891 grants (AH).

746

747

748

#### 749 **References**

- 750 Anders R, Alario F, Van Maanen L. 2016. The Shifted Wald Distribution for Response Time Data Analysis.  
751 *Psychol Methods* **21**:309–327.
- 752 Ando T. 2007. Bayesian predictive information criterion for the evaluation of hierarchical Bayesian and  
753 empirical Bayes models. *Biometrika* **94**:443–458. doi:10.1093/biomet/asm017
- 754 Apps MAJ, Lesage E, Ramnani N. 2015. Vicarious reinforcement learning signals when instructing others. *J*  
755 *Neurosci* **35**:2904–2913. doi:10.1523/JNEUROSCI.3669-14.2015
- 756 Arnold NR, Bröder A, Bayen UJ. 2015. Empirical validation of the diffusion model for recognition memory and  
757 a comparison of parameter-estimation methods. *Psychol Res* **79**:882–898. doi:10.1007/s00426-014-0608-y
- 758 Barto AG, Sutton RS, Brouwer PS. 1981. Associative search network: A reinforcement learning associative  
759 memory. *Biol Cybern* **40**:201–211. doi:10.1007/BF00453370



- 760 Bechara a, Damasio a R, Damasio H, Anderson SW. 1994. Insensitivity to future consequences following  
761 damage to human prefrontal cortex. *Cognition* **50**:7–15. doi:10.1016/0010-0277(94)90018-3
- 762 Behrens TEJ, Woolrich MW, Walton ME, Rushworth MFS. 2007. Learning the value of information in an  
763 uncertain world. *Nat Neurosci* **10**:1214–1221. doi:10.1038/nn1954
- 764 Boag RJ, Strickland L, Heathcote A, Neal A, Loft S. 2019a. Cognitive Control and Capacity for Prospective  
765 Memory in Complex Dynamic Environments. *J Exp Psychol Gen* **148**:2181–2206.  
766 doi:10.1037/xge0000599
- 767 Boag RJ, Strickland L, Loft S, Heathcote A. 2019b. Strategic attention and decision control support prospective  
768 memory in a complex dual-task environment. *Cognition* **191**:103974. doi:10.1016/j.cognition.2019.05.011
- 769 Bogacz R, Larsen T. 2011. Integration of reinforcement learning and optimal decision-making theories of the  
770 basal ganglia. *Neural Comput* **23**:817–851. doi:10.1162/NECO\_a\_00103
- 771 Bogacz R, McClure SM, Li J, Cohen JD, Montague PR. 2007. Short-term memory traces for action bias in  
772 human reinforcement learning. *Brain Res* **1153**:111–121. doi:10.1016/j.brainres.2007.03.057
- 773 Bogacz R, Wagenmakers E-J, Forstmann BU, Nieuwenhuis S. 2010. The neural basis of the speed-accuracy  
774 tradeoff. *Trends Neurosci* **33**:10–6. doi:10.1016/j.tins.2009.09.002
- 775 Boucher L, Palmeri TJ, Logan GD, Schall JD. 2007. Inhibitory Control in Mind and Brain : An Interactive Race  
776 Model of Countermanding Saccades **114**:376–397. doi:10.1037/0033-295X.114.2.376
- 777 Brooks SP, Gelman A. 1998. General Methods for Monitoring Convergence of Iterative Simulations. *J Comput*  
778 *Graph Stat* **7**:434–455. doi:10.1080/10618600.1998.10474787
- 779 Brown SD, Heathcote A. 2008. The simplest complete model of choice response time: Linear ballistic  
780 accumulation. *Cogn Psychol* **57**:153–178. doi:10.1016/j.cogpsych.2007.12.002
- 781 Christakou A, Gershman SJ, Niv Y, Simmons A, Brammer M, Rubia K. 2013. Neural and Psychological  
782 Maturation of Decision-making in Adolescence and Young Adulthood. *J Cogn Neurosci* **25**:1807–1823.  
783 doi:10.1162/jocn\_a\_00447
- 784 Cisek P, Puskas GA, El-Murr S. 2009. Decisions in changing conditions: the urgency-gating model. *J Neurosci*  
785 **29**:11560–71. doi:10.1523/JNEUROSCI.1844-09.2009
- 786 Collins AGE, Frank MJ. 2018. Within- and across-trial dynamics of human EEG reveal cooperative interplay  
787 between reinforcement learning and working memory. *Proc Natl Acad Sci* **115**:2502–2507.  
788 doi:10.1073/pnas.1720963115
- 789 Collins AGE, Frank MJ. 2012a. How much of reinforcement learning is working memory, not reinforcement  
790 learning? A behavioral, computational, and neurogenetic analysis. *Eur J Neurosci* **35**:1024–1035.  
791 doi:10.1111/j.1460-9568.2011.07980.x
- 792 Collins AGE, Frank MJ. 2012b. How much of reinforcement learning is working memory, not reinforcement  
793 learning? A behavioral, computational, and neurogenetic analysis. *Eur J Neurosci* **35**:1024–1035.  
794 doi:10.1111/j.1460-9568.2011.07980.x
- 795 Costa VD, Tran VL, Turchi J, Averbeck BB. 2015. Reversal learning and dopamine: A Bayesian perspective. *J*  
796 *Neurosci* **35**:2407–2416. doi:10.1523/JNEUROSCI.1989-14.2015
- 797 Daw ND, Dayan P. 2014. The algorithmic anatomy of model-based evaluation. *Philos Trans R Soc B Biol Sci*  
798 **369**. doi:10.1098/rstb.2013.0478
- 799 Daw ND, Kakade S, Dayan P. 2002. Opponent interactions between serotonin and dopamine. *Neural Networks*  
800 **15**:603–616. doi:10.1016/S0893-6080(02)00052-7
- 801 Daw ND, O’Doherty JP, Dayan P, Seymour B, Dolan RJ. 2006. Cortical substrates for exploratory decisions in  
802 humans. *Nature* **441**:876–879. doi:10.1038/nature04766
- 803 Dayan P, Daw ND. 2008. Decision theory, reinforcement learning, and the brain. *Cogn Affect Behav Neurosci*  
804 **8**:429–453. doi:10.3758/CABN.8.4.429
- 805 Donkin C, Brown SD. 2018. Response Times and Decision-Making, Stevens’ Handbook of Experimental  
806 Psychology and Cognitive Neuroscience. doi:10.1002/9781119170174.epcn509
- 807 Donkin C, Brown SD, Heathcote A. 2011. Drawing conclusions from choice response time models: A tutorial  
808 using the linear ballistic accumulator. *J Math Psychol* **55**:140–151. doi:10.1016/j.jmp.2010.10.001
- 809 Donkin C, Brown SD, Heathcote A. 2009. The overconstraint of response time models: Rethinking the scaling  
810 problem. *Psychon Bull Rev* **16**:1129–1135. doi:10.3758/PBR.16.6.1129
- 811 Dutilh G, Rieskamp J. 2016. Comparing perceptual and preferential decision making. *Psychon Bull Rev* **23**:723–  
812 737. doi:10.3758/s13423-015-0941-1
- 813 Fontanesi L, Gluth S, Spektor MS, Rieskamp J. 2019a. A reinforcement learning diffusion decision model for  
814 value-based decisions. *Psychon Bull Rev*. doi:10.3758/s13423-018-1554-2
- 815 Fontanesi L, Palminteri S, Lebreton M. 2019b. Decomposing the effects of context valence and feedback  
816 information on speed and accuracy during reinforcement learning: a meta-analytical approach using  
817 diffusion decision modeling. *Cogn Affect Behav Neurosci* **19**:490–502. doi:10.3758/s13415-019-00723-1
- 818 Forstmann BU, Ratcliff R, Wagenmakers E-J. 2016. Sequential Sampling Models in Cognitive Neuroscience:  
819 Advantages, Applications, and Extensions. *Annu Rev Psychol* **67**:641–666. doi:10.1146/annurev-psych-

- 820 122414-033645  
821 Frank MJ. 2004. By Carrot or by Stick: Cognitive Reinforcement Learning in Parkinsonism. *Science* (80- )  
822 **306**:1940–1943. doi:10.1126/science.1102941  
823 Frank MJ, Doll BB, Oas-Terpstra J, Moreno F. 2009. Prefrontal and striatal dopaminergic genes predict  
824 individual differences in exploration and exploitation. *Nat Neurosci* **12**:1062–1068. doi:10.1038/nn.2342  
825 Gelman A, Rubin DB. 1992. Inference from Iterative Simulation Using Multiple Sequences. *Stat Sci* **7**:457–472.  
826 doi:10.1214/ss/1177011136  
827 Gershman SJ. 2015. Do learning rates adapt to the distribution of rewards? *Psychon Bull Rev* **22**:1320–1327.  
828 doi:10.3758/s13423-014-0790-3  
829 Haughey HM, Hutchison KE, Curran T, Frank MJ, Moustafa AA. 2007. Genetic triple dissociation reveals  
830 multiple roles for dopamine in reinforcement learning. *Proc Natl Acad Sci* **104**:16311–16316.  
831 doi:10.1073/pnas.0706111104  
832 Hawkins GE, Forstmann BU, Wagenmakers E-J, Ratcliff R, Brown SD. 2015. Revisiting the Evidence for  
833 Collapsing Boundaries and Urgency Signals in Perceptual Decision-Making. *J Neurosci* **35**:2476–2484.  
834 doi:10.1523/JNEUROSCI.2410-14.2015  
835 Hawkins GE, Heathcote A. 2020. Racing Against The Clock: Evidence-Based Vs. Time-Based Decisions.  
836 *Psychol Rev*.  
837 Heathcote A, Lin YS, Reynolds A, Strickland L, Gretton M, Matzke D. 2019. Dynamic models of choice. *Behav*  
838 *Res Methods* **51**:961–985. doi:10.3758/s13428-018-1067-y  
839 Heathcote A, Love J. 2012. Linear deterministic accumulator models of simple choice. *Front Psychol* **3**:1–19.  
840 doi:10.3389/fpsyg.2012.00292  
841 Ho T, Brown SD, Van Maanen L, Forstmann BU, Wagenmakers E-J, Serences JT. 2012. The Optimality of  
842 Sensory Processing during the Speed-Accuracy Tradeoff. *J Neurosci* **32**:7992–8003.  
843 doi:10.1523/JNEUROSCI.0340-12.2012  
844 Izquierdo A, Brigman JL, Radke AK, Rudebeck PH, Holmes A. 2017. The neural basis of reversal learning: An  
845 updated perspective. *Neuroscience* **345**:12–26. doi:10.1016/j.neuroscience.2016.03.021  
846 Jang AI, Costa VD, Rudebeck PH, Chudasama Y, Murray EA, Averbeck BB. 2015. The role of frontal cortical  
847 and medial-temporal lobe brain areas in learning a Bayesian prior belief on reversals. *J Neurosci*  
848 **35**:11751–11760. doi:10.1523/JNEUROSCI.1594-15.2015  
849 Katsimpokis D, Hawkins GE, Van Maanen L. 2020. Not all Speed-Accuracy Trade-Off Manipulations Have the  
850 Same Psychological Effect. *Comput Brain Behav*. doi:10.1007/s42113-020-00074-y  
851 Leite FP, Ratcliff R. 2010. Modeling reaction time and accuracy of multiple-alternative decisions. *Attention,*  
852 *Perception, Psychophys* **72**:246–273. doi:10.3758/APP.72.1.246  
853 Logan GD, Van Zandt T, Verbruggen F, Wagenmakers EJ. 2014. On the ability to inhibit thought and action:  
854 General and special theories of an act of control. *Psychol Rev* **121**:66–95. doi:10.1037/a0035230  
855 Luzardo A, Alonso E, Mondragón E. 2017. A Rescorla-Wagner drift-diffusion model of conditioning and  
856 timing. *PLOS Comput Biol* **13**:e1005796. doi:10.1371/journal.pcbi.1005796  
857 McDougle SD, Collins AGE. 2020. Modeling the influence of working memory, reinforcement, and action  
858 uncertainty on reaction time and choice during instrumental learning. *Psychon Bull Rev*.  
859 doi:10.3758/s13423-020-01774-z  
860 Miletić S. 2016. Neural Evidence for a Role of Urgency in the Speed-Accuracy Trade-off in Perceptual  
861 Decision-Making. *J Neurosci* **36**:5909–5910. doi:10.1523/JNEUROSCI.0894-16.2016  
862 Miletić S, Boag RJ, Forstmann BU. 2020. Mutual benefits: Combining reinforcement learning with sequential  
863 sampling models. *Neuropsychologia* **136**. doi:10.1016/j.neuropsychologia.2019.107261  
864 Miletić S, Van Maanen L. 2019. Caution in decision-making under time pressure is mediated by timing ability.  
865 *Cogn Psychol* **110**:16–29. doi:10.1016/j.cogpsych.2019.01.002  
866 Millner AJ, Gershman SJ, Nock MK, den Ouden HEM. 2018. Pavlovian Control of Escape and Avoidance. *J*  
867 *Cogn Neurosci* **30**:1379–1390. doi:10.1162/jocn\_a\_01224  
868 Murphy PR, Boonstra E, Nieuwenhuis S. 2016. Global gain modulation generates time-dependent urgency  
869 during perceptual choice in humans. *Nat Commun* **7**:1–14. doi:10.1038/ncomms13526  
870 Niv Y, Edlund JA, Dayan P, O’Doherty JP. 2012. Neural Prediction Errors Reveal a Risk-Sensitive  
871 Reinforcement-Learning Process in the Human Brain. *J Neurosci* **32**:551–562.  
872 doi:10.1523/jneurosci.5498-10.2012  
873 O’Doherty JP, Cockburn J, Pauli WM. 2017. Learning, Reward, and Decision Making. *Annu Rev Psychol*  
874 **68**:73–100. doi:10.1146/annurev-psych-010416-044216  
875 Pachella RG, Pew RW. 1968. Speed-Accuracy Tradeoff in Reaction Time: Effect of Discrete Criterion Times. *J*  
876 *Exp Psychol* **76**:19–24. doi:10.1037/h0021275  
877 Palminteri S, Khamassi M, Joffily M, Coricelli G. 2015. Contextual modulation of value signals in reward and  
878 punishment learning. *Nat Commun* **6**. doi:10.1038/ncomms9096  
879 Palminteri S, Wyart V, Koehlin E. 2017. The Importance of Falsification in Computational Cognitive

- 880 Modeling. *Trends Cogn Sci* **21**:425–433. doi:10.1016/j.tics.2017.03.011
- 881 Pedersen ML, Frank MJ. 2020. Simultaneous Hierarchical Bayesian Parameter Estimation for Reinforcement  
882 Learning and Drift Diffusion Models: a Tutorial and Links to Neural Data. *Comput Brain Behav*.  
883 doi:10.1007/s42113-020-00084-w
- 884 Pedersen ML, Frank MJ, Biele G. 2017. The drift diffusion model as the choice rule in reinforcement learning.  
885 *Psychon Bull Rev* **24**:1234–1251. doi:10.3758/s13423-016-1199-y
- 886 Peirce J, Gray JR, Simpson S, MacAskill M, Höchenberger R, Sogo H, Kastman E, Lindeløv JK. 2019.  
887 PsychoPy2: Experiments in behavior made easy. *Behav Res Methods* **51**:195–203. doi:10.3758/s13428-  
888 018-01193-y
- 889 Purcell BA, Heitz RP, Cohen JY, Schall JD, Logan GD, Palmeri TJ. 2010. Neurally constrained modeling of  
890 perceptual decision making. *Psychol Rev* **117**:1113–1143. doi:10.1037/a0020311
- 891 Rae B, Heathcote A, Donkin C, Averell L, Brown SD. 2014. The hare and the tortoise: Emphasizing speed can  
892 change the evidence used to make decisions. *J Exp Psychol Learn Mem Cogn* **1**–39.  
893 doi:10.1037/a0036801
- 894 Ratcliff R. 1978. A theory of memory retrieval. *Psychol Rev* **85**:59–108.
- 895 Ratcliff R, Hasegawa YT, Hasegawa RP, Childers R, Smith PL, Segraves MA. 2011. Inhibition in superior  
896 colliculus neurons in a brightness discrimination task? *Neural Comput* **23**:1790–1820.  
897 doi:10.1162/NECO\_a\_00135
- 898 Ratcliff R, Hasegawa YT, Hasegawa RP, Smith PL, Segraves MA. 2007. Dual Diffusion Model for Single-Cell  
899 Recording Data From the Superior Colliculus in a Brightness-Discrimination Task. *J Neurophysiol*  
900 **97**:1756–1774. doi:10.1152/jn.00393.2006
- 901 Ratcliff R, McKoon G. 2008. The diffusion decision model: theory and data for two-choice decision tasks.  
902 *Neural Comput* **20**:873–922. doi:10.1162/neco.2008.12-06-420
- 903 Ratcliff R, Rouder JN. 1998. Modeling Response Times for Two-Choice Decisions. *Psychol Sci* **9**:347–356.
- 904 Ratcliff R, Smith PL, Brown SD, McKoon G. 2016. Diffusion Decision Model: Current Issues and History.  
905 *Trends Cogn Sci* **20**:260–281. doi:10.1016/j.tics.2016.01.007
- 906 Ratcliff R, Voskuilen C, Teodorescu A. 2018. Modeling 2-alternative forced-choice tasks: Accounting for both  
907 magnitude and difference effects. *Cogn Psychol* **103**:1–22. doi:10.1016/j.cogpsych.2018.02.002
- 908 Rescorla RA, Wagner AR. 1972. A theory of Pavlovian conditioning: Variations in the effectiveness of  
909 reinforcement and nonreinforcement. *Class Cond II Curr Res Theory* **21**:64–99.  
910 doi:10.1101/gr.110528.110
- 911 Rummery GA, Niranjan M. 1994. On-Line Q-Learning Using Connectionist Systems.
- 912 Sewell DK, Jach HK, Boag RJ, Van Heer CA. 2019. Combining error-driven models of associative learning  
913 with evidence accumulation models of decision-making. *Psychon Bull Rev*. doi:10.3758/s13423-019-  
914 01570-4
- 915 Sewell DK, Stallman A. 2020. Modeling the Effect of Speed Emphasis in Probabilistic Category Learning.  
916 *Comput Brain Behav* **3**:129–152. doi:10.1007/s42113-019-00067-6
- 917 Shahar N, Hauser TU, Moutoussis M, Moran R, Keramati M, Consortium NSPN, Dolan RJ. 2019. Improving  
918 the reliability of model-based decision-making estimates in the two-stage decision task with reaction-  
919 times and drift-diffusion modeling. *PLoS Comput Biol* **15**:1–25. doi:10.1371/journal.pcbi.1006803
- 920 Spektor MS, Kellen D. 2018. The relative merit of empirical priors in non-identifiable and sloppy models:  
921 Applications to models of learning and decision-making. *Psychon Bull Rev* **25**:2047–2068.  
922 doi:10.3758/s13423-018-1446-5
- 923 Spiegelhalter DJ, Best NG, Carlin BP, Van der Linde A. 2002. Bayesian measures of model complexity and fit.  
924 *J R Stat Soc Ser B (Statistical Methodol)* **64**:583–639.
- 925 Sutton, Richard S. 1988. Learning to Predict by the Method of Temporal Differences. *Mach Learn* **3**:9–44.  
926 doi:10.1023/A:1018056104778
- 927 Sutton RS, Barto AG. 2018. Reinforcement Learning: An Introduction, 2nd ed, MIT Press. Cambridge, MA:  
928 MIT press.
- 929 Teodorescu AR, Moran R, Usher M. 2016. Absolutely relative or relatively absolute: violations of value  
930 invariance in human decision making. *Psychon Bull Rev* **23**:22–38. doi:10.3758/s13423-015-0858-8
- 931 Ter Braak CJF. 2006. A Markov Chain Monte Carlo version of the genetic algorithm Differential Evolution:  
932 easy Bayesian computing for real parameter spaces. *Stat Comput* **16**:239–249. doi:10.1007/s11222-006-  
933 8769-1
- 934 Thura D, Cisek P. 2016. Modulation of Premotor and Primary Motor Cortical Activity during Volitional  
935 Adjustments of Speed-Accuracy Trade-Offs. *J Neurosci* **36**:938–956. doi:10.1523/JNEUROSCI.2230-  
936 15.2016
- 937 Tillman G, Van Zandt T, Logan GD. 2020. Sequential sampling models without random between-trial  
938 variability: the racing diffusion model of speeded decision making. *Psychon Bull Rev*.  
939 doi:10.3758/s13423-020-01719-6

- 940 Trueblood JS, Heathcote A, Evans NJ, Holmes WR. 2020. Urgency, Leakage, and the Relative Nature of  
941 Information Processing in Decision-making. *Psychol Rev* 706291. doi:10.1101/706291  
942 Turner BM. 2019. Toward a Common Representational Framework for Adaptation. *Psychol Rev*.  
943 doi:10.1037/rev0000148  
944 Turner BM, Sederberg PB, Brown SD, Steyvers M. 2013. A method for efficiently sampling from distributions  
945 with correlated dimensions. *Psychol Methods* **18**:368–384. doi:10.1037/a0032222  
946 van Maanen L, Miletic S. 2020. The interpretation of behavior-model correlations in unidentified cognitive  
947 models. *Psychon Bull Rev*. doi:10.3758/s13423-020-01783-y  
948 van Maanen L, van der Mijl R, van Beurden MHPH, Roijendijk LMM, Kingma BRM, Miletic S, van Rijn H.  
949 2019. Core body temperature speeds up temporal processing and choice behavior under deadlines. *Sci Rep*  
950 **9**:10053. doi:10.1038/s41598-019-46073-3  
951 Van Ravenzwaaij D, Brown SD, Marley AAJ, Heathcote A. 2020. Accumulating advantages: A new  
952 conceptualization of rapid multiple choice. *Psychol Rev* **127**:186–215. doi:10.1037/rev0000166  
953 Voss A, Nagler M, Lerche V. 2013. Diffusion models in experimental psychology: A practical introduction. *Exp*  
954 *Psychol* **60**:385–402. doi:10.1027/1618-3169/a000218  
955 Voss A, Rothermund K, Voss J. 2004. Interpreting the parameters of the diffusion model: An empirical  
956 validation. *Mem Cognit* **32**:1206–1220. doi:10.3758/BF03196893  
957